

Supporting Information

Fast synthesis of iridium(III) complexes with sulfur containing ancillary ligand for high-performance green OLEDs with EQE over 31%

Guang-Zhao Lu^{1,2#}, Zhen-Long Tu^{1,#}, Liang Liu¹, Wen-Wei Zhang,^{1,*} You-Xuan Zheng^{1,*}

¹*State Key Laboratory of Coordination Chemistry, Collaborative Innovation Center of Advanced Microstructures, Jiangsu Key Laboratory of Advanced Organic Materials, School of Chemistry and Chemical Engineering, Nanjing University, Nanjing 210093, P. R. China*

E-mail: wwzhang@nju.edu.cn, yxzheng@nju.edu.cn

²*Shenzhen Key Laboratory of Polymer Science and Technology, College of Materials Science and Engineering, Shenzhen University, Shenzhen 518060, P.R. China*

E-mail: gzhlu@szu.edu.cn

1. Materials and Measurements. All reagents and chemicals were purchased from commercial sources and used without further purification. ¹H NMR spectra were measured on a Bruker AM 400 spectrometer. Mass spectrometry (MS) spectra were obtained on an electrospray ionization (ESI) mass spectrometer (LCQ fleet, Thermo Fisher Scientific) for ligands and high-resolution electrospray mass spectra (HRMS) was measured on G6500 from Agilent for complexes. Elemental analyses for C, H, and N were performed on an Elementar Vario MICRO analyzer. TG-DSC measurements were carried out on a DSC 823e analyzer (METTLER). Absorption and photoluminescence spectra were measured on a UV-3100 spectrophotometer and a Hitachi F-4600 photoluminescence spectrophotometer, respectively. The decay lifetimes were measured with an Edinburgh Instruments FLS-920 fluorescence spectrometer in degassed CH₂Cl₂ solution at room temperature. The luminescence quantum efficiencies were calculated by comparison of the emission intensities (integrated areas) of a standard sample (*fac*-Ir(ppy)₃) and the unknown sample.¹

2. X-ray Crystallography. The single crystals of complexes were carried out on a Bruker SMART CCD diffractometer using monochromated Mo K α radiation ($\lambda = 0.71073 \text{ \AA}$) at room temperature. Cell parameters were retrieved using SMART software and refined using SAINT² on all observed reflections. Data were collected using a narrow-frame method with scan widths of 0.30° in ω and an exposure time of 10 s/frame. The highly redundant data sets

were reduced using SAINT and corrected for Lorentz and polarization effects. Absorption corrections were applied using SADABS³ supplied by Bruker. The structures were solved by direct methods and refined by full-matrix least-squares on *F*² using the program SHELXS-97.⁴ The positions of metal atoms and their first coordination spheres were located from direct-methods E-maps; other non-hydrogen atoms were found in alternating difference Fourier syntheses and least-squares refinement cycles and, during the final cycles, refined anisotropically. Hydrogen atoms were placed in calculated position and refined as riding atoms with a uniform value of Uiso.

3. Details of cyclic voltammetry measurements and theoretical calculations. Cyclic voltammetry measurements were conducted on a MPI-A multifunctional electrochemical and chemiluminescent system (Xi'an Remex Analytical Instrument Ltd. Co., China) at room temperature, with a polished Pt plate as the working electrode, platinum thread as the counter electrode and Ag-AgNO₃ (0.1 M) in CH₂Cl₂ as the reference electrode, *tetra-n*-butylammonium perchlorate (0.1 M) was used as the supporting electrolyte, using Fe⁺/Fc as the internal standard, the scan rate was 0.1 V/s. We perform theoretical calculations employing Gaussian09 software with B3LYP function.⁵ The basis set of 6-31G(d, p) was used for C, H, N, O, and F atoms while the LanL2DZ basis set was employed for Ir atoms.⁶ The solvent effect of CH₂Cl₂ was taken into consideration using conductor like polarizable continuum model (C-PCM).⁷

4. OLEDs fabrication and measurement. All OLEDs were fabricated on the pre-patterned ITO-coated glass substrate with a sheet resistance of 15 Ω/sq. The deposition rate for organic compounds is 1-2 Å/s. The phosphor and the host TCTA or 2,6DCzPPy were co-evaporated to form emitting layer from two separate sources. The cathode consisting of LiF / Al was deposited by evaporation of LiF with a deposition rate of 0.1 Å/s and then by evaporation of Al metal with a rate of 3 Å/s. The characteristic curves of the devices were measured with a computer which controlled KEITHLEY 2400 source meter with a calibrated silicon diode in air without device encapsulation. On the basis of the uncorrected PL and EL spectra, the Commission Internationale de l'Eclairage (CIE) coordinates were calculated using a test program of the Spectra scan PR650 spectrophotometer.

Table S1. The crystallographic data of $(4\text{tfmppy})_2\text{Ir}(\text{dipdtc})$, $(\text{TN}_4\text{T})_2\text{Ir}(\text{dipdtc})$ and $(24\text{btfmppy})_2\text{Ir}(\text{dipdtc})$.

| | $(4\text{tfmppy})_2\text{Ir}(\text{dipdtc})$ | $(24\text{btfmppy})_2\text{Ir}(\text{dipdtc})$ | $(\text{TN}_4\text{T})_2\text{Ir}(\text{dipdtc})$ |
|--|--|---|---|
| Formula | $\text{C}_{31}\text{H}_{28}\text{F}_6\text{IrN}_3\text{S}_2$ | $\text{C}_{33}\text{H}_{26}\text{F}_{12}\text{IrN}_3\text{S}_2$ | $\text{C}_{31}\text{H}_{24}\text{F}_{12}\text{IrN}_5\text{S}_2$ |
| Formula weight | 812.88 | 948.89 | 950.87 |
| T (K) | 296(2) | 293(2) | 153(2) |
| Wavelength (Å) | 0.71073 | 0.71073 | 0.71073 |
| Crystal system | Orthorhombic | Monoclinic | Monoclinic |
| Space group | Pbcn | P2 ₁ /n | C2/c |
| <i>a</i> (Å) | 15.7090(7) | 11.502(3) | 17.763(2) |
| <i>b</i> (Å) | 19.7575(9) | 18.947(4) | 11.7754(14) |
| <i>c</i> (Å) | 21.8169(9) | 16.970(4) | 17.580(2) |
| α (deg) | 90.00 | 90.00 | 90.00 |
| β (deg) | 90.00 | 98.420(4) | 103.941(2) |
| γ (deg) | 90.00 | 90.00 | 90.00 |
| <i>V</i> (Å ³) | 6771.3(5) | 3658.6(14) | 3568.8(7) |
| <i>Z</i> | 8 | 4 | 4 |
| ρ_{calcd} (g/cm ³) | 1.595 | 1.723 | 1.770 |
| μ (Mo K α) (mm ⁻¹) | 4.124 | 3.852 | 3.951 |
| <i>F</i> (000) | 3184 | 1848 | 1848 |
| Range of transm factors (deg) | 2.263-25.008 | 1.621-25.010 | 2.094-27.517 |
| Reflns collected | 46788 | 19913 | 11771 |
| Unique(R_{int}) | 5952(0.0355) | 6451(0.0484) | 4094(0.0579) |
| R_I^a, wR_2^b [$I > 2s(I)$] | 0.0212, 0.0506 | 0.0359, 0.0862 | 0.0451, 0.1015 |
| R_I^a, wR_2^b (all data) | 0.0287, 0.0547 | 0.0555, 0.0996 | 0.0600, 0.1099 |
| GOF on <i>F</i> ² | 1.075 | 1.093 | 1.021 |
| CCDC number | 1832358 | 1832332 | 1832370 |

$$R_I^a = \Sigma ||F_o| - |F_c|| / \Sigma |F_o|. \quad wR_2^b = [\Sigma w(F_o^2 - F_c^2)^2 / \Sigma w(F_o^2)]^{1/2}.$$

Table S2. Selected bond lengths and angles of $(4\text{tfmppy})_2\text{Ir}(\text{dipdtc})$, $(\text{TN}_4\text{T})_2\text{Ir}(\text{dipdtc})$ and $(24\text{btfmppy})_2\text{Ir}(\text{dipdtc})$.

| | $(4\text{tfmppy})_2\text{Ir}(\text{dipdtc})$ | $(24\text{btfmppy})_2\text{Ir}(\text{dipdtc})$ | $(\text{TN}_4\text{T})_2\text{Ir}(\text{dipdtc})$ |
|-----------------|--|--|---|
| Selected bonds | Bond length (Å) | Bond length (Å) | Bond length (Å) |
| Ir-C(1) | 2.010(3) | 2.081(6) | 2.015(5) |
| Ir-C(2) | 2.015(3) | 2.0804(52) | 2.019(5) |
| Ir-N(1) | 2.055(3) | 2.060(5) | 2.036(5) |
| Ir-N(2) | 2.047(2) | 2.060(5) | 2.029(5) |
| Ir-S(1) | 2.4552(7) | 2.4195(17) | 2.4381(15) |
| Ir-S(2) | 2.4456(8) | 2.4195(17) | 2.4501(16) |
| S(1)-C(3) | 1.735(3) | 1.746(6) | 1.728(6) |
| S(2)-C(3) | 1.723(3) | 1.746(6) | 1.719(5) |
| C(3)-N(3) | 1.323(4) | 1.318(14) | 1.333(7) |
| Selected angles | (°) | (°) | (°) |
| C(1)-Ir-N(1) | 80.2(11) | 80.7(2) | 79.5(2) |
| C(2)-Ir-N(2) | 80.24(11) | 80.7(2) | 79.0(2) |
| S(1)-Ir-S(2) | 71.36(3) | 72.31(8) | 71.64(5) |
| S(2)-C(3)-S(1) | 111.50(18) | 109.6(5) | 112.2(3) |
| C(3)-S(2)-Ir | 88.74(11) | 89.005(71) | 88.0(2) |
| C(3)-S(1)-Ir | 88.18(11) | 89.0(3) | 88.16(18) |
| N(3)-C(3)-S(1) | 123.5(2) | 125.2(3) | 124.4(4) |

Table S3. The electronic cloud density distribution.

| Complex | Orbital | Energy/eV | Energy/eV | Composition (%) | | |
|---|---------|--------------|----------------|-----------------|-------|-------------------|
| | | (Calculated) | (Experimental) | Main Ligands | Ir | Ancillary Ligands |
| $(4\text{tfmppy})_2\text{Ir}(\text{dipdtc})$ | HOMO | -5.45 | -5.25 | 47.90 | 48.18 | 8.79 |
| | LUMO | -1.77 | -2.80 | 92.83 | 3.94 | 3.23 |
| $(24\text{btfmppy})_2\text{Ir}(\text{dipdtc})$ | HOMO | -5.70 | -5.47 | 38.95 | 48.54 | 12.51 |
| | LUMO | -2.08 | -3.12 | 94.61 | 3.42 | 1.97 |
| $(\text{TN}_4\text{T})_2\text{Ir}(\text{dipdtc})$ | HOMO | -5.97 | -5.76 | 31.53 | 45.11 | 23.37 |
| | LUMO | -2.12 | -3.24 | 94.04 | 2.88 | 3.08 |

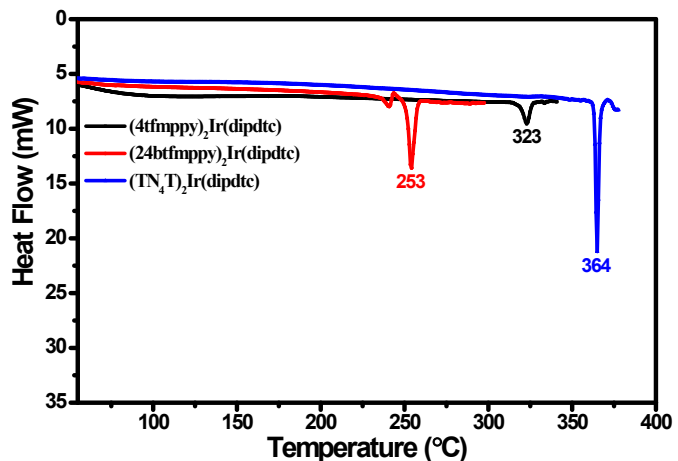


Fig. S1 The DSC spectra of the iridium(III) complexes.

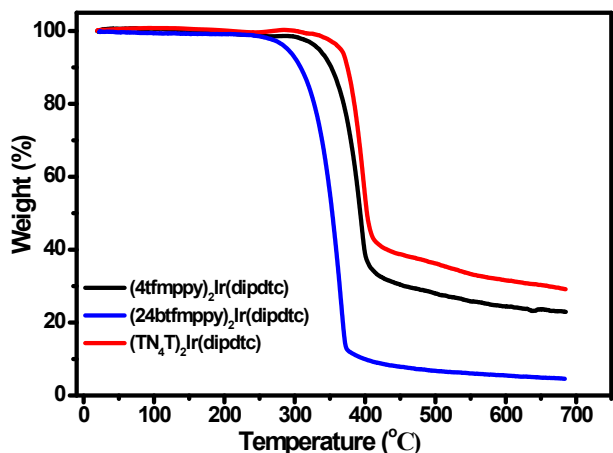


Fig. S2 The TG curves of the iridium(III) complexes.

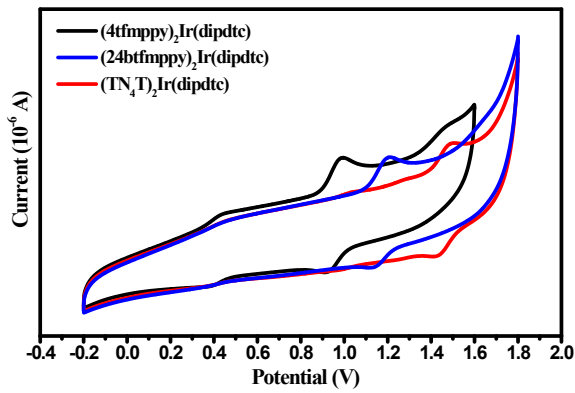


Fig. S3 Cyclic voltammogram curves of complexes the iridium(III) complexes.

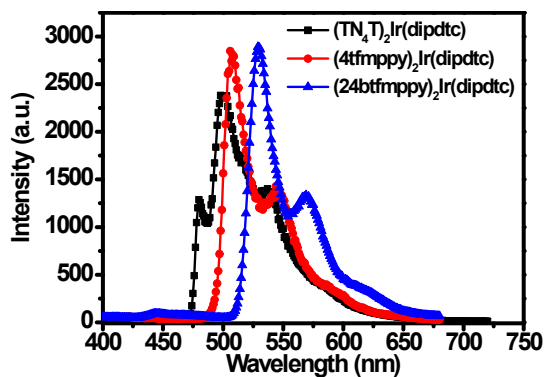


Fig. S4 The emission spectra of the iridium(III) complexes at 77 K in CH_2Cl_2 solution.

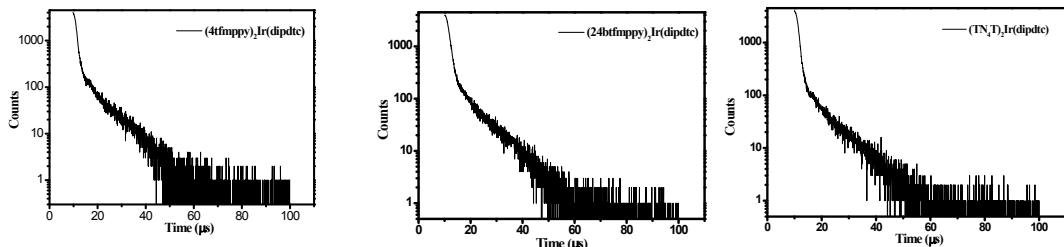


Fig. S5 The selected lifetime curves of the iridium(III) complexes in degassed CH_2Cl_2 solution.

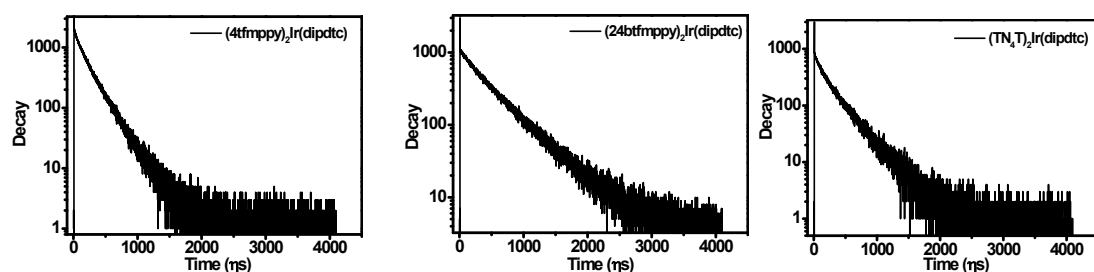


Fig. S6 The selected lifetime curves of the iridium(III) complexes in 5 wt% doped TCTA films.

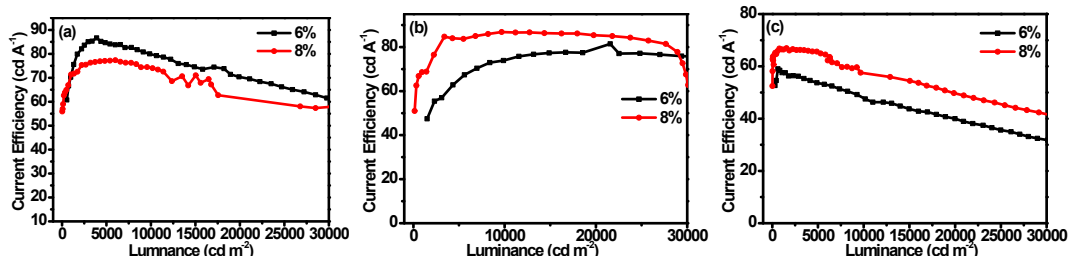


Fig. S7 Current efficiency versus luminance of different doped concentrations for double-emitting-layer devices: (a) $(\text{TN}_4\text{T})_2\text{Ir}(\text{dipdtc})$, (b) $(4\text{tfmpy})_2\text{Ir}(\text{dipdtc})$ and (c) $(24\text{btfmppy})_2\text{Ir}(\text{dipdtc})$.

References:

1. D. P. Rillema, D. G. Taghdiri, D. S. Jones, C. D. Keller, L. A. Worl, T. J. Meyer and H. A. Levy, *Inorg. Chem.*, 1987, **26**, 578.
2. *SAINT-Plus*, version 6.02, Bruker Analytical X-ray System, Madison, WI, 1999.
3. Sheldrick, G. M. *SADABS An empirical absorption correction program*, Bruker Analytical X-ray Systems, Madison, WI, 1996.
4. Sheldrick, G. M. *SHELXTL-97*. Universität of Göttingen, Göttingen, Germany, 1997.
5. E. Runge and E. K. U. Gross, *Phys. Rev. Lett.*, 1984, **52**, 997.
6. M. J. Frisch, G. W. Trucks, H. B. Schlegel, G. E. Scuseria, M. A. Robb, J. R. Cheeseman, G. Scalmani, V. Barone, B. Mennucci, G. A. Petersson, H. Nakatsuji, M. Caricato, X. Li, H. P. Hratchian, A. F. Izmaylov, J. Bloino, G. Zheng, J. L. Sonnenberg, M. Hada, M. Ehara, K. Toyota, R. Fukuda, J. Hasegawa, M. Ishida, T. Nakajima, Y. Honda, O. Kitao, H. Nakai, T. Vreven, J. A. Montgomery Jr., J. E. Peralta, F. Ogliaro, M. Bearpark, J. J. Heyd, E. Brothers, K. N. Kudin, V. N. Staroverov, R. Kobayashi, J. Normand, K. Raghavachari, A. Rendell, J. C. Burant, S. S. Iyengar, J. Tomasi, M. Cossi, N. Rega, J. M. Millam, M. Klene, J. E. Knox, J. B. Cross, V. Bakken, C. Adamo, J. Jaramillo, R. Gomperts, R. E. Stratmann, O. Yazyev, A. J. Austin, R. Cammi, C. Pomelli, J. W. Ochterski, R. L. Martin, K. Morokuma, V. G. Zakrzewski, G. A. Voth, P. Salvador, J. J. Dannenberg, S. Dapprich, A. D. Daniels, O. Farkas, J. B. Foresman, J. V. Ortiz, J. Cioslowski, D. J. Fox, Gaussian 09, Revision A.01, Gaussian, Inc., Wallingford, CT, 2009.
7. (a) P. J. Hay and W. R. Wadt, *J. Chem. Phys.*, 1985, **82**, 299; (b) M. M. Franklin, W. J. Pietro, W. J. Hehre, J. S. Binkley, M. S. Gordon, D. J. Defrees and J. A. Pople, *J. Chem. Phys.*, 1982, **77**, 3654.